scientific reports

Check for updates

OPEN

Plants exposed to titanium dioxide nanoparticles acquired contrasting photosynthetic and morphological strategies depending on the growing light intensity: a case study in radish

Akram Vatankhah[1,2], Sasan Aliniaeifard[1]✉, Moein Moosavi-Nezhad[1,3], Sahar Abdi[1], Zakieh Mokhtarpour[1], Saeed Reezi[2], Georgios Tsaniklidis[4] & Dimitrios Fanourakis[5]

Due to the photocatalytic property of titanium dioxide (TiO_2), its application may be dependent on the growing light environment. In this study, radish plants were cultivated under four light intensities (75, 150, 300, and 600 µmol m^{-2} s^{-1} photosynthetic photon flux density, PPFD), and were weekly sprayed (three times in total) with TiO_2 nanoparticles at different concentrations (0, 50, and 100 µmol L^{-1}). Based on the obtained results, plants used two contrasting strategies depending on the growing PPFD. In the first strategy, as a result of exposure to high PPFD, plants limited their leaf area and send the biomass towards the underground parts to limit light-absorbing surface area, which was confirmed by thicker leaves (lower specific leaf area). TiO_2 further improved the allocation of biomass to the underground parts when plants were exposed to higher PPFDs. In the second strategy, plants dissipated the absorbed light energy into the heat (NPQ) to protect the photosynthetic apparatus from high energy input due to carbohydrate and carotenoid accumulation as a result of exposure to higher PPFDs or TiO_2 concentrations. TiO_2 nanoparticle application up-regulated photosynthetic functionality under low, while down-regulated it under high PPFD. The best light use efficiency was noted at 300 m^{-2} s^{-1} PPFD, while TiO_2 nanoparticle spray stimulated light use efficiency at 75 m^{-2} s^{-1} PPFD. In conclusion, TiO_2 nanoparticle spray promotes plant growth and productivity, and this response is magnified as cultivation light intensity becomes limited.

Abbreviations

ABS/RC	The specific energy fluxes per reaction center for energy absorption
DI_0/RC	The dissipated energy flux
ET_0/RC	The electron transport flux per reaction center
F_m	The maximum fluorescence when all PSII reaction centers are closed
F_v	The variable fluorescence of the dark-adapted sample
F_v/F_m	Ratio of variable to maximum fluorescence
FW	Fresh weight
F_0	The minimum fluorescence when all PSII reaction centers are open
LMR	Leaf mass ratio

[1]Photosynthesis Laboratory, Department of Horticulture, Aburaihan Campus, University of Tehran, P.O. Box 33916-53755, Tehran, Iran. [2]Department of Horticulture, Faculty of Agriculture, University of Shahrekord, Shahrekord, Iran. [3]Department of Horticultural Sciences, North Carolina State University, Raleigh, NC 27695, USA. [4]Laboratory of Vegetable Crops, Institute of Olive Tree, Subtropical Plants and Viticulture, Hellenic Agricultural Organization 'ELGO DIMITRA', 73100 Chania, Greece. [5]Laboratory of Quality and Safety of Agricultural Products, Landscape and Environment, Department of Agriculture, School of Agricultural Sciences, Hellenic Mediterranean University, Estavromenos, 71004 Heraklion, Greece. ✉email: aliniaeifard@ut.ac.ir

NPQ	Non-photochemical quenching
PI_{ABS}	The performance index in light absorption basis
PPFD	Photosynthetic photon flux density
PSII	Photosystem II
rETR	Relative electron transport rate
SLA	Specific leaf area
TEM	Transmission electron microscopy
TiO_2	Titanium dioxide
TMR	Tuber mass ratio
TR_0/RC	The trapped energy flux per reaction center
XRD	X-ray diffraction
$\Delta F/F_{m'}$	Effective quantum yield of PSII
φ_{D0}	The quantum yield of energy dissipation
Φ_{PSII}	Effective quantum yield of PSII
φ_{E0}	The quantum yield of electron transport
φ_{PAV}	The quantum yield for primary photochemistry

Global food demand is steadily rising as a result of a growing population[1]. To ensure global food security, further improvements in crop yields are necessary[1,2]. Intensifying agricultural production by increasing the associated inputs is commonly employed as an effective strategy to stimulate plant growth and performance[3–6]. Yet, improving input use efficiency stands out as a more attractive alternative[6], since the intensification-associated environmental pressure is evaded[7].

Noteworthy, the application of nanoparticles has proven to be a powerful tool in advancing yield[8]. For instance, the application of titanium dioxide (TiO_2) nanoparticles has been associated with stimulation of carbohydrate production, chlorophyll formation, as well as improvements in photosynthetic rate and eventually yield[9,10]. These promotive effects are concentration dependent, and vary excessively among species[9,11]. In addition, the positive effect of TiO_2 nanoparticles on plant growth and productivity depends on the environmental conditions during cultivation[10,11]. In this regard, their application may be exercised when the remaining conditions allow optimal impact on plants. For instance, plant growth and productivity also strongly depends on light availability[12–15]. Light is the main energy source-driver of photosynthesis. Light intensity is the pivotal determinant of plant growth and performance[16–18]. Production of crops in greenhouses and controlled environments has nowadays attracted a lot of attention[19]. There is a need to optimize the photosynthetic photon flux density (PPFD) needed for plant growth in an approach with the highest resource use efficiency[6,18]. TiO_2 nanoparticles are used to improvemeyield during winter cultivation of plants[20]. However, the effect of either TiO_2 nanoparticles application or light level has been limitedly addressed. It, therefore, remains unknown whether or not these two factors interact to determine plant yield.

Chlorophyll fluorescence is often employed for non-invasive assessments of the electron transport system properties[21–24]. Polyphasic chlorophyll fluorescence induction curves may be additionally utilized to study the fate of absorbed light energy and provide further insights into the structure and function of the photosynthetic system[25–27].

TiO_2 nanoparticles have special properties such as high specific area, easy operation, high absorption capacity, and photocatalytic activity. They have emerged as antimicrobial agents and growth promoters. Chahardoli et al.[28], showed that promoting effects of TiO_2 application on the growth of plants are concentration-dependent. Indeed, in low concentrations (50 and 100 mg L^{-1}) TiO_2 nanoparticles had a stimulating effect; while increasing the concentration to 2500 mg L^{-1} impose an inhibitory effect on plant growth[24]. It has been reported that TiO_2 nanoparticles increase the rate of photosynthesis and plant immunity, leading to a 30% increase in yield[11]. In the study of Hossein et al.[29], foliar application of 2.5 mg L^{-1} Ti, chlorophyll pigments (chlorophyll a, b, carotenoid), plant biomass, photochemical efficiency of photosystem II (F_v/F_m) and electron transfer rate (ETR) of soybean improve under natural light conditions. Choi et al.[30] reported that TiO_2 foliar application affected CO_2 absorption and chlorophyll fluorescence of cherry tomato plants. Foliar spraying of TiO_2 during cloudy days with low light intensity increased the electron transfer rate from Q_A to Q_B in the reaction center of photosystem II (ET_0/RC) and carbon dioxide (CO_2) stabilization. The use of TiO_2 nanoparticles for strawberry cultivation in the winter, which is characterized by low light intensity, increased the chlorophyll content, fruit yield, and firmness of strawberry fruit[20].

Controlled environment agriculture (CEA) has emerged as a new sustainable approach to increase the productivity of crops irrespective of natural environmental variations[27]. However, increasing the efficacy of artificial light in CEA is of vital importance to make it energy-cost effective[31]. There is scarce information on the interaction of light intensity and TiO_2 nanoparticles in the CEA. Considering that TiO_2 nanoparticles have photocatalytic activity, they can be capable of increasing the efficiency of light use[32]. Therefore, detailed information on their practical impacts on photosynthesis and crop growth is needed.

The aim of this study was to investigate for the first time the joint inputs of cultivation light level and TiO_2 nanoparticles application on determining photosynthetic efficiency, biomass allocation and yield in controlled-environment agriculture. Radish (*Raphanus raphanistrum* L.) was employed as a model species, owing to the high harvest index (i.e., edible leaves and tuber), and short growth cycle[33]. The obtained data serve as a conceptual basis for understanding the approaches that plants utilized under different scenarios of light energy inputs, as well as for the stimulation of photosynthetic capacity with the aim of maximizing plant growth and productivity, especially in indoor environments where light use efficiency is of obvious concern.

Results

Characterization of TiO_2. The surface morphology of TiO_2 nanoparticles was determined by scanning electron microscope (SEM) and transmission electron microscopy (TEM) (Fig. 1A–D). Briefly, TiO_2 nanoparticles were spherical or rod-shaped with -32 mV zeta potential and good dispersion. The size of most nanoparticles was in the range of 10–25 (average 18 nm) nm. Using BET method, SSA, pore volume, and average pore diameter were evaluated as 69.679 m^2g^{-1}, 0.2588 cm^3g^{-1}, and 14.857 nm, respectively.

X-ray diffraction showed all diffraction peaks of the anatase phase well (Fig. 1E). The characteristic peak of the anatase phase was $2\Theta = 25.3$[34]. Several sharp peaks are observed in the 2Θ range at 20–80°. The sharp peaks in the 2Θ range were 25.12°, 38.25°, 48.10°, 54°, 55.1°, 63°, 69.0°, 70.50°, and 75.10°.

The FTIR spectrum of TiO_2 nanoparticles is shown in Fig. 1F. The used spectrometer has measured vibrations in the wavelength range of 350–4000 cm^{-1}. The broad peak at 3411.46 cm^{-1} was related to the intermolecular interaction of the hydroxyl group (−OH) attached to Ti. The 1629.55 peak corresponds to the -OH bending vibration. The broad peak at 452.225 cm^{-1} is assigned to the bending vibration bonds (Ti–O–Ti) in the TiO_2 lattice[34]. The observation of the mentioned peaks in the FTIR spectrum indicates the presence of Ti in the nanoparticle structure and the formation of TiO_2 nanoparticles.

In present study, TiO_2 foliar application affected chlorophyll fluorescence parameters of radish plants under different light intensities. Our results showed that foliar spraying of TiO_2 nanoparticles reduced the negative

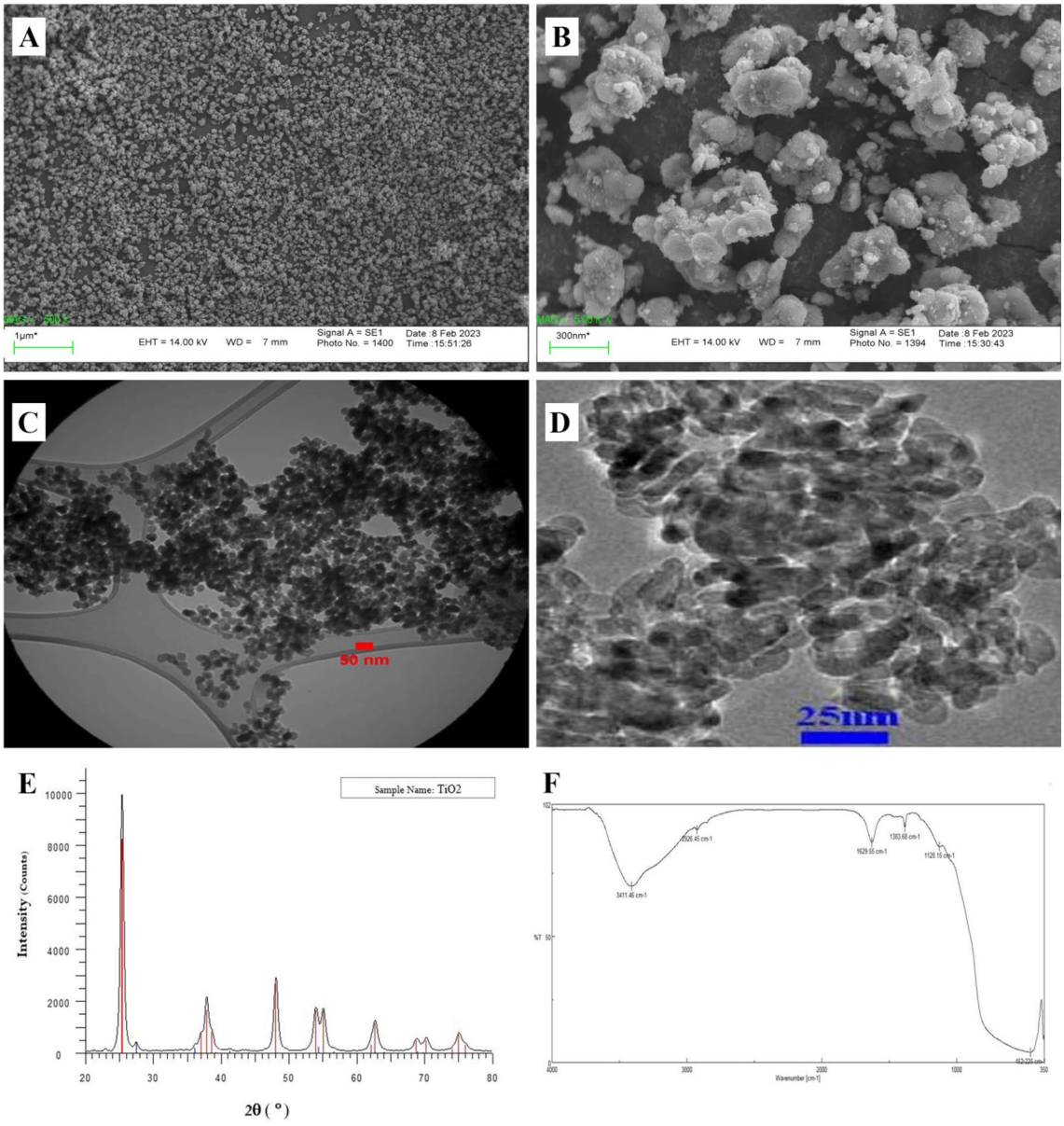

Figure 1. Representative scanning electron microscope (SEM), transmission electron microscopy (TEM) images (**A**–**D**), X-ray diffraction (XRD) pattern (**E**), and fourier-transform infrared spectroscopy (**F**) of titanium dioxide (TiO_2) nanoparticles employed in the present study.

influence of low light intensity on radish. TiO_2 treatment led to an increase in EI_0/RC under low light conditions, which indicates that TiO_2 improves the rate of electron transfer flux in photosystem II reaction centers. In addition, in the reaction center of TiO_2-treated plants, the dissipated energy flux DI_0/RC decreased, indicating that TiO_2 contributed to the photosynthetic light response.

Increasing cultivation light intensity improved plant growth, and triggered biomass allocation towards the tuber in a TiO_2 concentration-dependent manner. Plants were cultivated under four light intensities (75, 150, 300 and 600 μmol m^{-2} s^{-1} PPFD), and weekly sprayed with three TiO_2 nanoparticle levels (0, 50, and 100 μmol L^{-1}).

An increase in cultivation light intensity from 75 to 150 μmol m^{-2} s^{-1} PPFD resulted in a two-fold plant leaf area (Table 1; see also Fig. 2). This increase was mostly due to larger individual leaf area, and secondarily due to an increase in leaf number. A two-step increase in cultivation light intensity from 150 (though 300) to 600 μmol m^{-2} s^{-1} PPFD led to a smaller increase in plant leaf area. This increase was exclusively related to an increase in leaf number.

At 75, 150, and 300 μmol m^{-2} s^{-1} PPFD, TiO_2 nanoparticle spray stimulated plant leaf area (Table 1; see also Fig. 2). This increase was exclusively related to an increase in individual leaf area. At 150 μmol m^{-2} s^{-1} PPFD, the low TiO_2 nanoparticle level (50 μmol L^{-1}) was optimal for plant leaf area, while at 75 and 300 μmol m^{-2} s^{-1} PPFD no significant difference was noted among the two TiO_2 nanoparticle levels. At 600 μmol m^{-2} s^{-1} PPFD, the low TiO_2 nanoparticle level (50 μmol L^{-1}) did not affect plant leaf area, while the high TiO_2 nanoparticle level (100 μmol L^{-1}) decreased it. This decrease was exclusively related to a decrease in leaf number.

Increasing cultivation light intensity resulted in shorter leaf petioles (Table 1). Within each light intensity, TiO_2 nanoparticle spray decreased leaf petiole in a concentration-dependent manner in all cases, besides one (150 μmol m^{-2} s^{-1} PPFD, 100 μmol L^{-1}).

Increasing cultivation light intensity strongly stimulated plant dry weight (Table 1; see also Fig. 2). For instance, plant dry weight was 0.15 g at 75 μmol m^{-2} s^{-1} PPFD, while it was 1.86 g at 600 μmol m^{-2} s^{-1} PPFD. This increase in plant dry weight was mediated via respective increases in both shoot and tuber dry weights.

At each cultivation light intensity, TiO_2 nanoparticle spray stimulated plant dry weight (Table 1; see also Fig. 2). No significant difference was noted between the two TiO_2 nanoparticle levels.

Increasing cultivation light intensity generally led to thinner leaves (i.e., lower SLA; Table 1). At 75 μmol m^{-2} s^{-1} PPFD, TiO_2 nanoparticle spray was also associated with thinner leaves (Table 1). At 300 μmol m^{-2} s^{-1} PPFD, the opposite trend was noted (Table 1).

Increasing cultivation light intensity generally decreased dry mass allocation to leaves, and increased dry mass allocation to the tuber (Table 1; Fig. 3). At 300 and 600 μmol m^{-2} s^{-1} PPFD, this trend was magnified by TiO_2 nanoparticle spray in a TiO_2 concentration-dependent manner (Table 1; Fig. 3).

Increasing cultivation light intensity generally improved leaf chlorophyll and carotenoid contents in a TiO_2 concentration-dependent manner. Increasing cultivation light intensity up to 300 μmol m^{-2} s^{-1} PPFD led to an increase in leaf chlorophyll and carotenoid contents, while a further increase to 600 μmol m^{-2} s^{-1} PPFD resulted in a respective decrease (Fig. 4).

TiO_2 nanoparticle spray generally stimulated leaf chlorophyll content, and counteracted the noted decrease at 600 μmol m^{-2} s^{-1} PPFD (Fig. 4A).

Light intensity (μmol m^{-2} s^{-1})	TiO_2 (μmol L^{-1})	Leaf			Petiole length (leaf $^{-1}$)	Dry weight (g)			Tuber volume (mL)	SLA (cm^2 g^{-1})	LMR (g g^{-1})	TMR (g g^{-1})
		Number (plant^{-1})	Area (cm^2 leaf^{-1})	Area (cm^2 plant^{-1})		Shoot	Tuber	Plant				
75	0	4.0^{d}	11.0^{d}	43.9^{f}	7.11^{a}	0.09^{e}	0.07^{f}	0.15^{f}	1.50^{d}	520^{a}	0.56^{ab}	0.44^{de}
	50	4.0^{d}	17.9^{abc}	71.5^{e}	5.47^{bcd}	0.16^{d}	0.11^{f}	0.27^{ef}	1.00^{d}	447^{ab}	0.60^{a}	0.40^{e}
	100	4.0^{d}	16.8^{c}	67.3^{e}	5.88^{bc}	0.17^{d}	0.13^{f}	0.30^{ef}	1.00^{d}	403^{b}	0.56^{ab}	0.44^{de}
150	0	4.7^{bcd}	18.3^{abc}	85.2^{cd}	6.37^{ab}	0.22^{cd}	0.21^{ef}	0.43^{e}	2.00^{d}	415^{b}	0.50^{bc}	0.50^{cd}
	50	5.3^{ab}	20.8^{abc}	109.8^{a}	4.93^{cde}	0.42^{b}	0.37^{de}	0.79^{d}	9.50^{c}	262^{c}	0.53^{ab}	0.47^{de}
	100	4.3^{cd}	21.9^{ab}	93.4^{bc}	7.79^{a}	0.25^{c}	0.57^{d}	0.81^{d}	2.50^{d}	383^{b}	0.30^{d}	0.70^{b}
300	0	5.7^{a}	16.7^{c}	94.0^{bc}	4.91^{cde}	0.43^{b}	0.56^{d}	0.99^{d}	2.00^{d}	223^{cde}	0.43^{c}	0.57^{c}
	50	5.0^{abc}	21.9^{ab}	110^{a}	3.92^{ef}	0.43^{b}	0.89^{c}	1.31^{c}	9.50^{c}	258^{cd}	0.33^{d}	0.67^{b}
	100	5.0^{abc}	22.6^{a}	110^{a}	3.77^{ef}	0.41^{b}	1.11^{b}	1.52^{c}	8.50^{c}	271^{c}	0.27^{de}	0.73^{ab}
600	0	5.7^{a}	17.8^{bc}	100^{ab}	4.39^{def}	0.55^{a}	1.32^{b}	1.86^{b}	19.0^{b}	186^{de}	0.30^{d}	0.70^{b}
	50	5.3^{ab}	19.4^{abc}	103^{ab}	3.29^{gf}	0.57^{a}	1.58^{a}	2.14^{a}	25.0^{a}	182^{e}	0.27^{de}	0.73^{ab}
	100	4.3^{cd}	19.0^{abc}	76.9^{de}	2.17^{g}	0.44^{b}	1.74^{a}	2.18^{a}	19.0^{b}	177^{e}	0.20^{e}	0.80^{a}

Table 1. Effect of cultivation light intensity and spray treatment (once a week, and three times in total) with titanium dioxide (TiO_2) nanoparticles on growth and morphology of radish cv. Cherry belle plants. Six replicate plants were assessed per treatment. In traits, where the interaction of the two factors (light intensity, TiO_2 nanoparticle concentration) was significant, different letters indicate significant differences. *LMR* leaf mass ratio, *SLA* specific leaf area, *TMR* tuber mass ratio.

Figure 2. The growth environment (top panels), and representative images of radish cv. Cherry belle plants cultivated under different light intensities and sprayed (once a week, and three times in total) with titanium dioxide (TiO_2) nanoparticles at different levels.

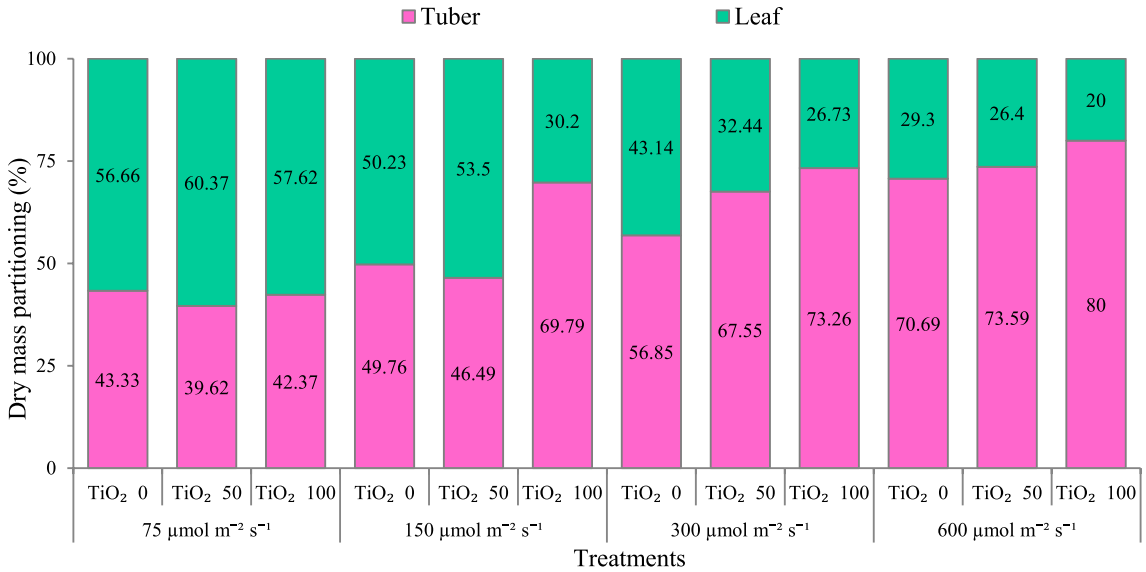

Figure 3. Effect of cultivation light intensity (75, 150, 300 and 600 µmol m^{-2} s^{-1}) and spray treatment (once a week, and three times in total) with titanium dioxide (TiO_2) nanoparticles (0, 50 and 100 µmol L^{-1}) on biomass partitioning of radish cv. Cherry belle plants. Six replicate plants were assessed per treatment.

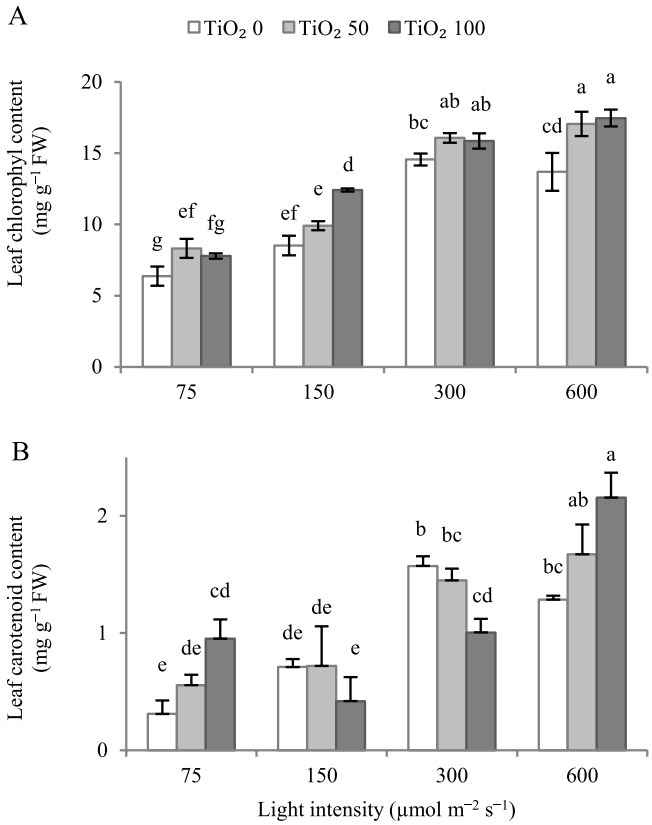

Figure 4. Effect of cultivation light intensity (75, 150, 300 and 600 µmol m^{-2} s^{-1}) and spray treatment (once a week, and three times in total) with titanium dioxide (TiO_2) nanoparticles (open, grey, and dark grey for 0, 50 and 100 µmol L^{-1}, respectively) on leaf chlorophyll, and carotenoid contents of radish cv. Cherry belle plants. Six replicate plants were assessed per treatment. Bars represent SEM. In traits, where the interaction of the two factors (light intensity, TiO_2 nanoparticle level) was significant, different letters indicate significant differences. FW, fresh weight.

At 75, and 600 µmol m^{-2} s^{-1} PPFD, TiO_2 nanoparticle spray stimulated leaf carotenoid content, and counteracted the noted decrease at 600 µmol m^{-2} s^{-1} PPFD (Fig. 4B). At 150, and 300 µmol m^{-2} s^{-1} PPFD, the high TiO_2 nanoparticle level (100 µmol L^{-1}) tended to decrease leaf carotenoid content, with this effect being only significant at 300 µmol m^{-2} s^{-1} PPFD.

Increasing cultivation light intensity and applying TiO_2 nanoparticles generally induce accumulation of soluble carbohydrates in both leaves and tuber. Increasing cultivation light intensity above 150 µmol m^{-2} s^{-1} PPFD tended to increase leaf total soluble carbohydrates content, with this effect being only significant at 600 µmol m^{-2} s^{-1} PPFD (Fig. 5A). At 300, and 600 µmol m^{-2} s^{-1} PPFD, the high TiO_2 nanoparticle level (100 µmol L^{-1}) stimulated leaf total soluble carbohydrates content.

Increasing cultivation light intensity enhanced tuber total soluble carbohydrates content (Fig. 5B). At 75, 150, and 300 µmol m^{-2} s^{-1} PPFD, TiO_2 nanoparticle spray generally stimulated tuber total soluble carbohydrates content.

TiO_2 nanoparticle application up-regulated photosynthetic functionality under low cultivation light intensity, while down-regulated photosynthetic functionality under high cultivation light intensity. At the lowest cultivation intensity (75 µmol m^{-2} s^{-1} PPFD), the lowest F_v/F_m was noted (Fig. 6). At the highest cultivation intensity (600 µmol m^{-2} s^{-1} PPFD), intermediate F_v/F_m values were apparent, with the highest ones being noted at 150, and 300 µmol m^{-2} s^{-1} PPFD.

At 75, and 150 µmol m^{-2} s^{-1} PPFD, TiO_2 nanoparticle spray stimulated F_v/F_m (Fig. 6). At 300 µmol m^{-2} s^{-1} PPFD, the high TiO_2 nanoparticle level (100 µmol L^{-1}) promoted F_v/F_m. At 600 µmol m^{-2} s^{-1} PPFD, TiO_2 nanoparticle spray decreased F_v/F_m.

Increasing the cultivation light intensity generally decreased the minimum fluorescence when all PSII reaction centers are open (F_0; Fig. 7A). At 75 µmol m^{-2} s^{-1} PPFD, TiO_2 nanoparticle spray decreased F_0.

Increasing the cultivation light intensity generally decreased the maximum fluorescence when all PSII reaction centers are closed (F_m; Fig. 7B) and the variable fluorescence of the dark-adapted sample (F_v; Fig. 7C). Within each light intensity regime, TiO_2 nanoparticle spray did not have any effect on F_m and F_v.

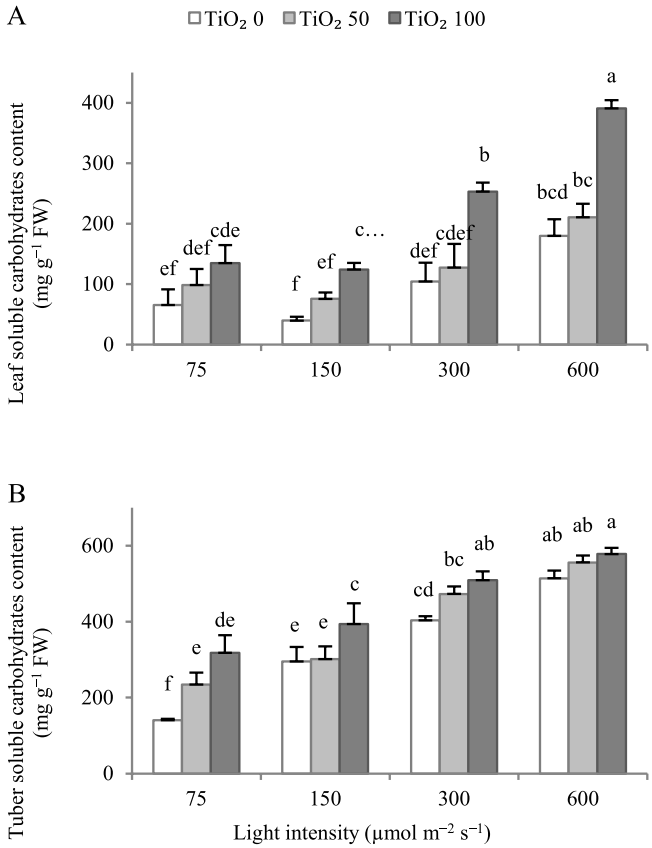

Figure 5. Effect of cultivation light intensity (75, 150, 300 and 600 µmol m^{-2} s^{-1}) and spray treatment (once a week, and three times in total) with titanium dioxide (TiO_2) nanoparticles (open, grey, and dark grey for 0, 50 and 100 µmol L^{-1}, respectively) on total carbohydrates content in leaves and tuber (**A**,**B**, respectively) of radish cv. Cherry belle plants. Six replicate plants were assessed per treatment. Bars represent SEM. In traits, where the interaction of the two factors (light intensity, TiO_2 nanoparticle level) was significant, different letters indicate significant differences. The difference in the y-axis scale among panels ought to be noted. FW, fresh weight.

F_v/F_m was higher at 150 and 300 µmol m^{-2} s^{-1} PPFD, as compared to 75 µmol m^{-2} s^{-1} PPFD (Fig. 7D). TiO_2 nanoparticle spray increased F_v/F_m at 75 µmol m^{-2} s^{-1} PPFD.

Cultivation light intensity did not affect the quantum yield of electron transport (φ_{E0}; Fig. 8A) and the performance index in light absorption basis (PI_{ABS}; Fig. 8D). TiO_2 nanoparticle spray increased φ_{E0} and PI_{ABS} at 75 µmol m^{-2} s^{-1} PPFD.

The quantum yield of energy dissipation (φ_{D0}) was higher at 75 µmol m^{-2} s^{-1} PPFD as compared to 150 and 300 µmol m^{-2} s^{-1} PPFD (Fig. 8B). TiO_2 nanoparticle spray decreased φ_{D0} at 75 µmol m^{-2} s^{-1} PPFD.

Increasing the cultivation intensity generally decreased the quantum yield for primary photochemistry (φ_{PAV}; Fig. 8C). TiO_2 nanoparticle spray decreased φ_{PAV} at 75 µmol m^{-2} s^{-1} PPFD.

Increasing cultivation light intensity generally decreased the specific energy fluxes per reaction center for energy absorption (ABS/RC; Fig. 9A), and the trapped energy flux per reaction center (TR_0/RC; Fig. 9B). TiO_2 nanoparticle spray decreased ABS/RC at 75 µmol m^{-2} s^{-1} PPFD (Fig. 9A).

The electron transport flux per reaction center (ET_0/RC) was lower at 600 µmol m^{-2} s^{-1} PPFD as compared to lower intensities (Fig. 9C). TiO_2 nanoparticle spray did not affect ET_0/RC.

The dissipated energy flux (DI_0/RC) was higher at 75 µmol m^{-2} s^{-1} PPFD as compared to higher light intensities (Fig. 9D). TiO_2 nanoparticle spray decreased DI_0/RC at 75 µmol m^{-2} s^{-1} PPFD (Fig. 9D). At 0 µmol m^{-2} s^{-1} PPDF measuring light intensity, ΦPSII was not affected by cultivation light intensity (Fig. 10A). As measuring light intensity increased, ΦPSII decreased. Leaves cultivated under higher light intensities generally sustained higher ΦPSII values across measurement light levels (100–1000 µmol m^{-2} s^{-1} PPFD). At 75 µmol m^{-2} s^{-1} PPFD during cultivation, the high TiO2 nanoparticle level (100 µmol L–1) tended to sustain higher ΦPSII values. As measurement light intensity increased, rETR also increased (Fig. 10B). Differences among cultivation light intensities were magnified, as measurement light intensity increased. The lower rETR was noted in leaves cultivated under 75 µmol m–2 s–1 PPFD.

Increasing cultivation light intensity and applying TiO_2 nanoparticles generally stimulate non-photochemical quenching. The non-photochemical quenching (NPQ) was higher at 600 µmol m^{-2} s^{-1} PPFD as compared to lower light intensities (Fig. 11). TiO_2 nanoparticle spray generally

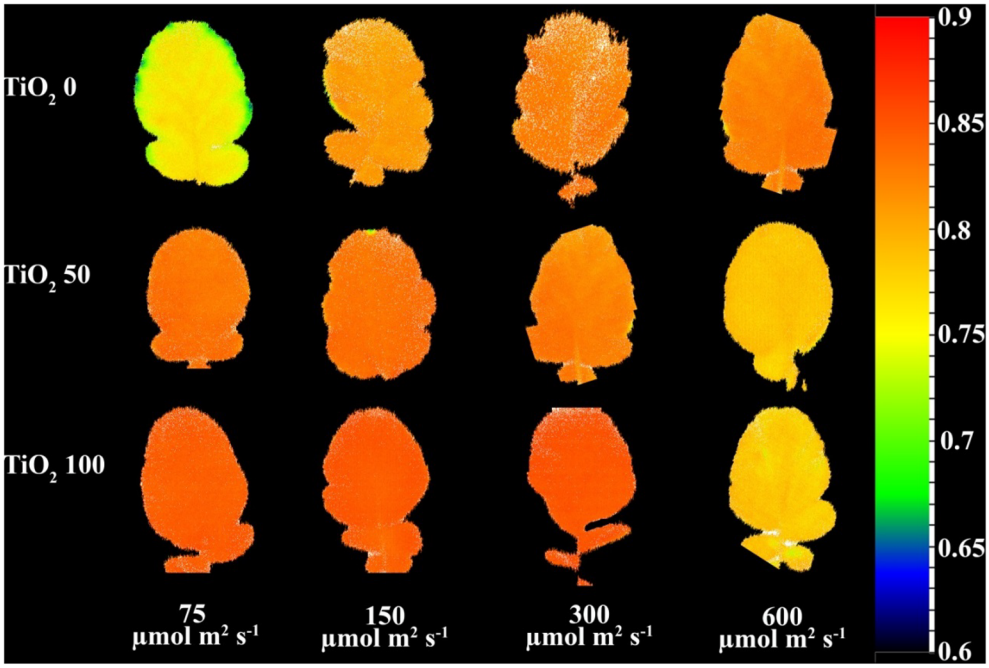

Figure 6. Representative image of the maximal quantum yield of PSII photochemistry (F_v/F_m) (equation and explanation in Table 3) of radish cv. Cherry belle plants cultivated under different light intensities (75, 150, 300 and 600 µmol m^{-2} s^{-1}) and sprayed (once a week, and three times in total) with titanium dioxide (TiO_2) nanoparticles at different concentrations (0, 50 and 100 µmol L^{-1}).

increased NPQ across cultivation light intensities. This effect was comparable at different cultivation light intensities.

Discussion

In this study, the optimal concentration (50, and 100 µmol L^{-1}) of TiO_2 nanoparticles foliar application for stimulating photosynthetic efficiency, and eventually yield was evaluated in radish. There are some previous indications highlighting more effectiveness of the foliar application of TiO_2 nanoparticles on crop growth, photosynthesis, and yield. For instance, the application of TiO_2 nanoparticles (average diameter 25 nm, in the form of anatase, zeta potentials -22.5 mV) in aerosol format was more effective compared to TiO_2 nanoparticles as a soil amendment for increasing photosynthesis and lycopene content[35]. The dependence of the respective promotive effect on cultivation light intensity (75, 150, 300 and 600 µmol m^{-2} s^{-1} PPFD) was also investigated in the present study.

Increasing cultivation light intensity resulted in a larger plant leaf area (Table 1; see also Fig. 2), and in this way improved light capture[36]. The plant leaf area increase was most prominent when light intensity increased from 75 to 150 µmol m^{-2} s^{-1} PPFD, while a further increase in light intensity led to a more moderate (plant leaf area) increase. In the former case (from 75 to 150 µmol m^{-2} s^{-1} PPFD), the increase in plant leaf area was mostly due to larger individual leaf area, whereas in the latter case (≥ 300 µmol m^{-2} s^{-1} PPFD), it was exclusively due to the larger number of leaves (thus enhanced leaf initiation). Therefore, the initial light level (rather than the percentage of increase) strongly determines both the promoting effect of increasing light intensity on plant leaf area, and the underlying process by which this increase is realized (i.e., individual leaf area and/ or the number of leaves).

When cultivation light intensity did not exceed 300 µmol m^{-2} s^{-1} PPFD, TiO_2 nanoparticle spray also stimulated plant leaf area (Table 1; see also Fig. 2). The TiO_2 nanoparticle spray-induced increase in plant leaf area was due to increased individual leaf area. The TiO_2 nanoparticle spray-induced increase in plant leaf area was more prominent as cultivation light intensity was lower. Therefore, applying TiO_2 nanoparticles provides an additional advantage in plants cultivated at low light levels.

Increasing cultivation light intensity resulted in larger plant biomass (Table 1; see also Fig. 2). The applied light levels (75–600 m^{-2} s^{-1} PPFD) were thus below the light saturation point of the crop[12]. The light intensity-induced increase in plant biomass was more prominent as the initial light intensity was lower. Across cultivation light intensities, TiO_2 nanoparticle spray stimulated plant biomass (Table 1; see also Fig. 2). The TiO_2 nanoparticle application-induced increase in plant biomass was also more prominent as the cultivation light intensity was lower. Both TiO_2 nanoparticle levels (50, and 100 µmol L^{-1}) were equally effective in stimulating plant biomass.

More plant mass was allocated to the leaves (i.e., higher LMR), as cultivation light intensity was lower (Table 1; Fig. 3). Thus, plants favored biomass partitioning to the light-intercepting organ (leaves) to amplify carbon gain under low light level conditions, whereas this partitioning gradually shifted to the tuber, which is evidently affiliated with the supply of other resources (i.e., water and nutrients), under higher light level circumstances[12]. Fine-tuning of leaf thickness (SLA) by regulating the light capture surface was another important aspect of adaptation to the light level in radish. Leaves were consistently thinner (i.e., higher SLA) as the light level decreased

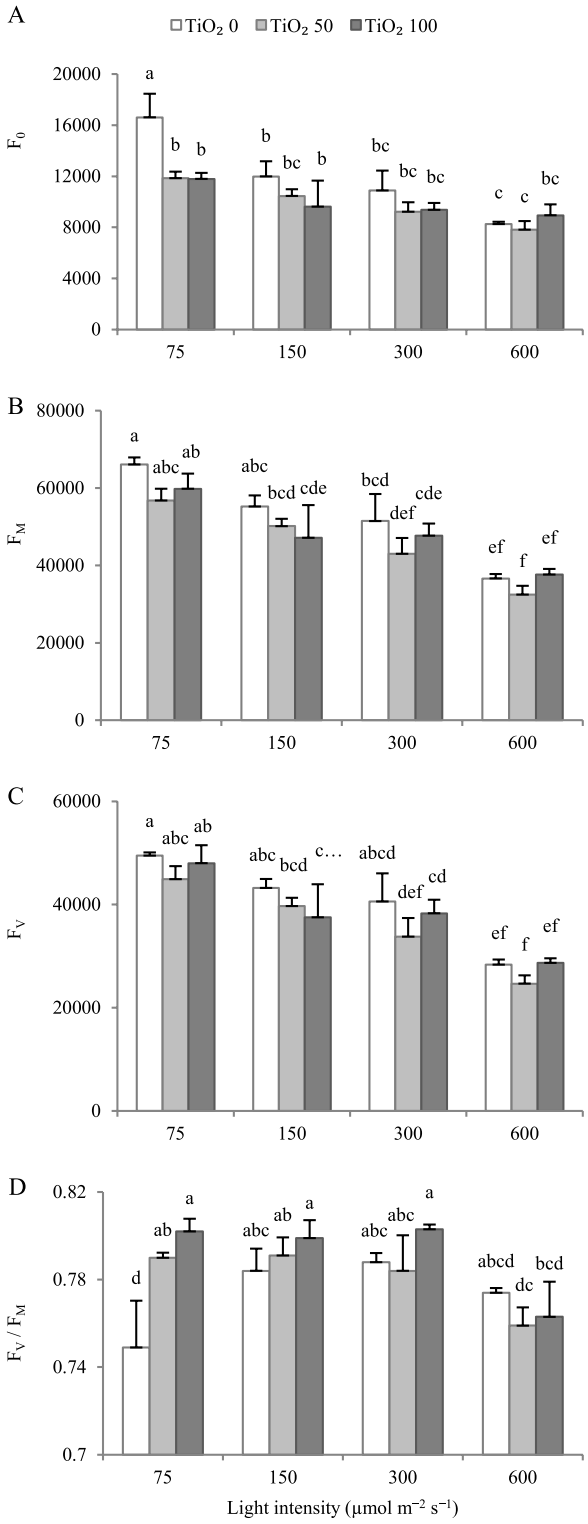

Figure 7. Effect of cultivation light intensity (75, 150, 300 and 600 µmol m^{-2} s^{-1}) and spray treatment (once a week, and three times in total) with titanium dioxide (TiO_2) nanoparticles (open, grey, and dark grey for 0, 50 and 100 µmol L^{-1}, respectively) on minimum fluorescence when all PSII reaction centers are open (F_0; **A**), maximum fluorescence when all PSII reaction centers are closed (F_m; **B**), variable fluorescence of the dark-adapted sample (F_v; **C**) and maximal quantum yield of PSII photochemistry (F_v/F_m; **D**) (equations and explanations in Table 3) of radish cv. Cherry belle plants. Nine replicate plants were assessed per treatment. Bars represent SEM. In traits, where the interaction of the two factors (light intensity, TiO_2 nanoparticle level) was significant, different letters indicate significant differences.

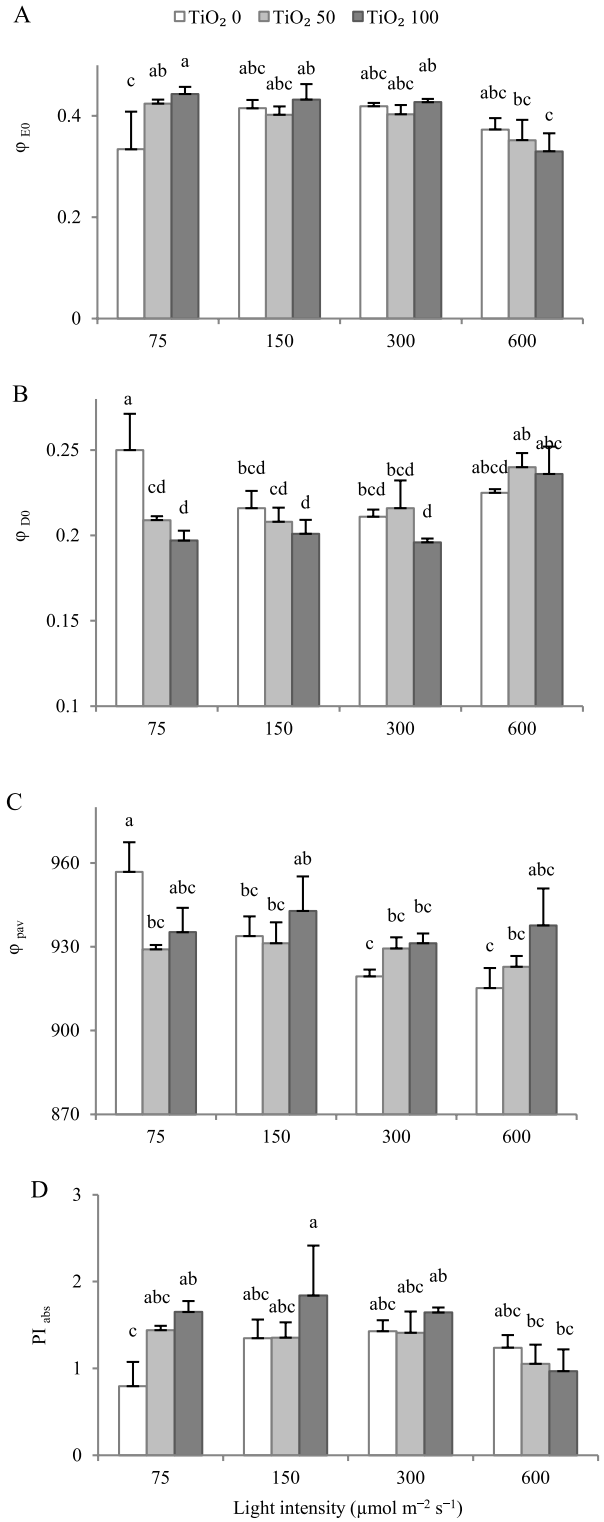

Figure 8. Effect of cultivation light intensity (75, 150, 300 and 600 μmol m^{-2} s^{-1}) and spray treatment (once a week, and three times in total) with titanium dioxide (TiO_2) nanoparticles (open, grey, and dark grey for 0, 50 and 100 μmol L^{-1}, respectively) on quantum yield of electron transport (φ_{E0}; **A**), quantum yield of energy dissipation (φ_{D0}; **B**), quantum yield for primary photochemistry (φ_{PAV}; **C**), performance index in light absorption basis (PI_{ABS}; **D**) (equations and explanations in Table 3) of radish cv. Cherry belle plants. Nine replicate plants were assessed per treatment. Bars represent SEM. In traits, where the interaction of the two factors (light intensity, TiO_2 nanoparticle level) was significant, different letters indicate significant differences.

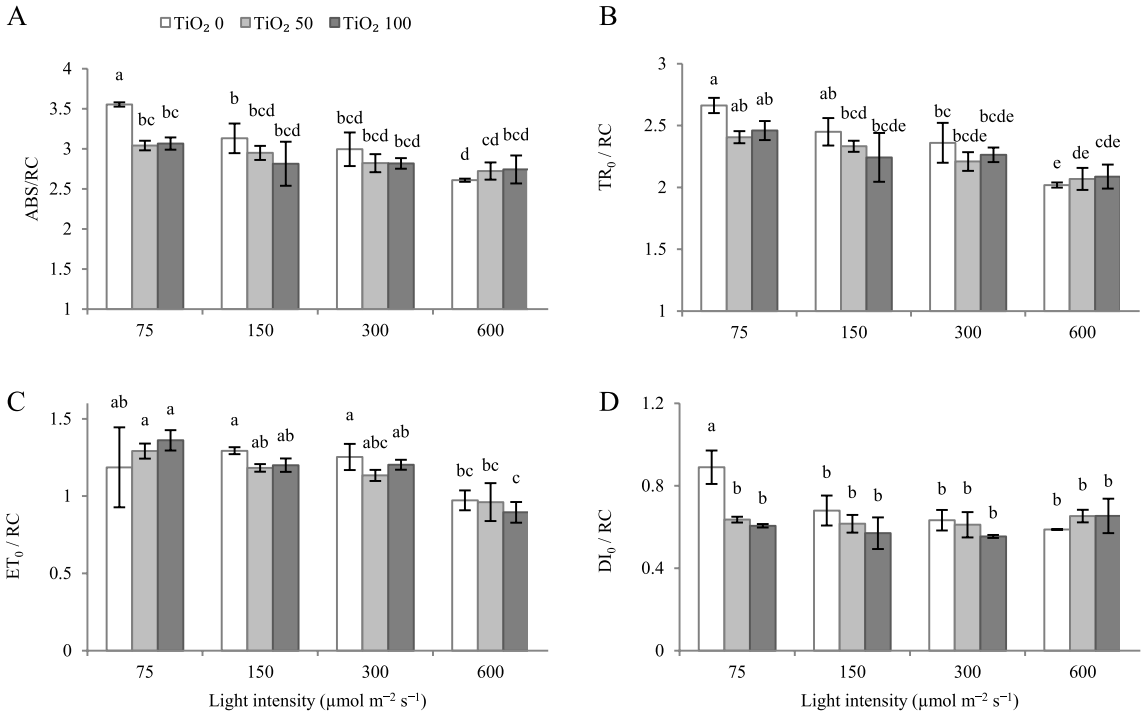

Figure 9. Effect of cultivation light intensity (75, 150, 300 and 600 μmol m^{-2} s^{-1}) and spray treatment (once a week, and three times in total) with titanium dioxide (TiO_2) nanoparticles (open, grey, and dark grey for 0, 50 and 100 μmol L^{-1}, respectively) on specific energy fluxes per reaction center for energy absorption (ABS/RC; **A**), trapped energy flux per reaction center (TR_0/RC; **B**), electron transport flux per reaction center (ET_0/RC; **C**), dissipated energy flux (DI_0/RC; **D**) (equations and explanations in Table 3) of radish cv. Cherry belle plants. Nine replicate plants were assessed per treatment. Bars represent SEM. In traits, where the interaction of the two factors (light intensity, TiO_2 nanoparticle level) was significant, different letters indicate significant differences.

(Table 1). Increasing SLA stimulates the amount of light which is intercepted, and in this way maximizes carbon assimilation. This adaptation in leaf morphology is common in low-light situations, and has been reported in several taxa[12].

Throughout the distribution chain of edible greens, the intensity of leaf greenness is an index of quality[5]. At inadequate leaf chlorophyll level, photosynthetic efficiency is also impeded[23]. Carotenoids are the main antioxidant metabolites, contributing to plant defense, and exhibiting health-promoting properties when consumed[5]. Increasing cultivation light intensity up to 300 μmol m^{-2} s^{-1} PPFD improved both leaf chlorophyll and carotenoid contents, while a further increase (600 μmol m^{-2} s^{-1} PPFD) exerted an adverse effect (Fig. 4). At 75, 150, and 600 μmol m^{-2} s^{-1} PPFD, TiO_2 nanoparticle spray promoted leaf chlorophyll content (Fig. 4A). At 75, and 600 μmol m^{-2} s^{-1} PPFD, TiO_2 nanoparticle spray also enhanced leaf carotenoid content (Fig. 4B). In either case, the optimum TiO_2 nanoparticle concentration depended on light level. Therefore, applying TiO_2 nanoparticles improves both leaf chlorophyll and carotenoid contents, especially under extreme light environments (i.e., low or very high).

Increasing cultivation light intensity generally stimulated the content of total soluble carbohydrates (primary energy reserves) in both leaves and tuber, with this effect being more prominent in the tuber (Fig. 5). TiO_2 nanoparticle spray further improved both leaf and tuber total soluble carbohydrates contents, with this effect being more pronounced in the leaf (Fig. 5). The level of primary energy reserves has been earlier associated with prolonged postharvest longevity[22,37]. For instance, an increased content of soluble carbohydrates may support maintenance needs (by sustaining ATP synthesis), and protect membrane integrity (by scavenging reactive oxygen species)[22,37].

Growth environment determines the light energy absorbance by the PSII apparatus, and this is readily reflected by chlorophyll fluorescence analysis[38]. As growth PPFD increased, a decreasing trend was noted in the F_0, F_m, and F_v (Fig. 7A–C). These parameters (F_0, F_m, and F_v) were generally not affected by TiO_2 nanoparticle spray, except for a decrease in F_0 at 75 μmol m^{-2} s^{-1} PPFD. The decrease in F_0 may be associated with a reduction in plastoquinone electron receptors and incomplete oxidation due to retardation, which results in electron transfer chain postponement in PSII. Alternatively, F_0 may be decreased by the separation of light-harvesting Chl a/b protein complexes in PSII[39]. The reduction in F_m is probably related to the deactivation of proteins in chlorophyll structure.

Higher values of F_v/F_m [$(F_m - F_0)/F_m$; Table 3] reflect a better light use efficiency[39]. Under stress, both the rising trend of F_0 and the declining trend of F_m typically underlie the decrease in F_v/F_m[15,25,40]. This decline in F_v/F_m denotes a stress-induced damage in the structure or function of PSII. As growth PPFD increased up to 300 μmol m^{-2} s^{-1} PPFD, F_v/F_m also increased (Fig. 7D; see also Fig. 6). A further increase in growth PPFD to

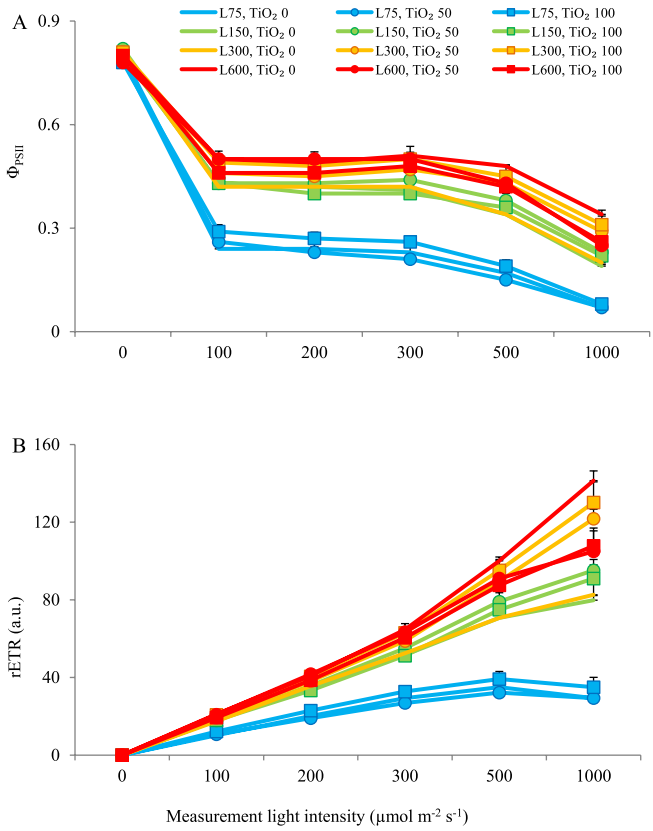

Figure 10. Rapid light curve of effective quantum yield of PSII (Φ_{PSII}, **A**) and electron transport rate (rETR, **B**) (equations and explanations in Table 3) as a function of measurement light intensity in radish cv. Cherry belle plants cultivated under different light intensities (75, 150, 300 and 600 µmol m^{-2} s^{-1}) and sprayed (once a week, and three times in total) with titanium dioxide (TiO_2) nanoparticles at different concentrations (0, 50 and 100 µmol L^{-1}). Nine replicate plants were assessed per treatment. Bars represent SEM.

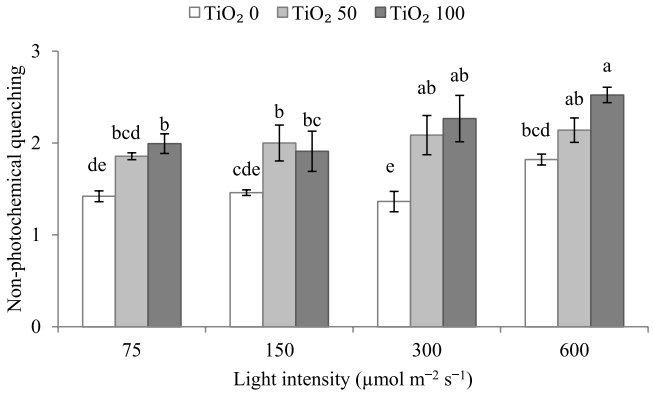

Figure 11. Effect of cultivation light intensity (75, 150, 300 and 600 µmol m^{-2} s^{-1}) and spray treatment (once a week, and three times in total) with titanium dioxide (TiO_2) nanoparticles (open, grey, and dark grey for 0, 50 and 100 µmol L^{-1}, respectively) on non-photochemical quenching (equation and explanation in Table 3) of radish cv. Cherry belle plants. Nine replicate plants were assessed per treatment. Bars represent SEM. The interaction of the two factors (light intensity, TiO_2 nanoparticle level) was significant, and different letters indicate significant differences.

600 µmol m^{-2} s^{-1} led to a decrease in F_v/F_m. Therefore, the optimum growth light intensity for light use efficiency was clearly the 300 µmol m^{-2} s^{-1} PPFD. In lettuce, the optimum growth light intensity was 600 µmol m^{-2} s^{-1} PPFD[16,17,41–44], while for *Aloe vera* L. it was 50% of sunlight as compared to 75 or 100%[44]. F_v/F_m was generally not affected by TiO_2 nanoparticle spray, except for an increase noted at 75 µmol m^{-2} s^{-1} PPFD. Therefore, TiO_2 nanoparticle spray improved light use efficiency at the lowest growth light intensity.

PI_{ABS} is an index of the quantum yield of absorbed photons, and is highly sensitive to changes in the concentration of reaction centers, initial photochemistry, and electron transport[14,45]. Exposure to non-optimal PPFD leads to alterations in absorption and energy trapping, thereby adversely influencing PI_{ABS}[17]. Similarly to F_v/F_m, PI_{ABS} increased as growth PPFD increased up to 300 µmol m^{-2} s^{-1} PPFD, and then (600 µmol m^{-2} s^{-1} PPFD) slightly decreased (Fig. 8D). Likewise to F_v/F_m, TiO_2 nanoparticle spray increased PI_{ABS} at 75 µmol m^{-2} s^{-1} PPFD. A decrease in PI_{ABS} may be due to the higher light energy absorption, dissipated energy flux, and lower electron transport per reaction center (expressed by ABS/RC, DI_0/RC, and ET_0/RC, respectively)[46].

ABS/RC flux is divided into TR_0/RC, ET_0/RC, and DI_0/RC, while the share of ABS is converted to DI and TR. As growth PPFD increased, ABS/RC tended to decrease (Fig. 9A). ABS/RC was generally not affected by TiO_2 nanoparticle spray, except for a decrease apparent at 75 µmol m^{-2} s^{-1} PPFD. The decreasing trend in ABS/RC indicates the more efficient function of the electron transport system, which decreases the excitation force on each reaction center and directs that energy mostly toward photosystem I.

At 600 µmol m^{-2} s^{-1} PPFD, ET_0/RC was lower (Fig. 9C), indicating an adverse effect in the rate of electron transport flux on PSII reaction centers. Increasing cultivation light intensity generally decreased TR_0/RC (Fig. 9B). At 75 µmol m^{-2} s^{-1} PPFD, DI_0/RC was higher (Fig. 9D). These parameters (ET_0/RC, TR_0/RC, and DI_0/RC) were generally not affected by TiO_2 nanoparticle spray, except a decrease in DI_0/RC at 75 µmol m^{-2} s^{-1} PPFD. A high DI_0/RC is generally associated with decreased F_v/F_m and an increased incidence of photoinhibition[17,47]. Since DI_0/RC is related to the partial deactivation of PSII reaction centers, it usually increases when PSII reaction centers cannot transfer energy upstream of PSII as a consequence of damage to the thylakoid membrane[14,48]. Shabbir et al.[49] reported that the photochemical efficiency of PSII increased by applying 90 mg L^{-1} TiO_2 to vetiver plants. In the study by Gao et al.[50] treatment of spinach with TiO_2 resulted in the induction of a complex of Rubisco and Rubisco activase to accelerate the carboxylation of Rubisco and ultimately improve photosynthetic efficiency. In the study of Azmat et al.[51], the treatment of spinach with TiO_2 nanoparticles increased the starch content due to its photocatalytic properties.

The absorbed light energy is quenched via photochemistry, fluorescence, or heat dissipation. In a healthy photosystem, a large portion is used to perform photosynthesis (the so-called photochemical quenching), and a trivial one is released via fluorescence. The third fate is NPQ, in which the excess excitation energy of the chlorophyll in the PSII complex is harmlessly dissipated into thermal energy[52]. Therefore, NPQ signifies an effective way for dissipating excessive irradiation into heat by the photosynthetic apparatus[53]. Studying the behavior of NPQ provides information regarding the xanthophyll cycle activity and other energy-quenching pathways which are induced by the proton concentration inside thylakoids[54–56]. NPQ was higher at 600 µmol m^{-2} s^{-1} PPFD (Fig. 11). Across cultivation light intensities, TiO_2 nanoparticle spray generally increased NPQ. Thus, it can be concluded that plants grown under the highest PPFD and/ or TiO_2 nanoparticle spray directed more efficiently the excess excitation energy through non-radiative dissipative processes. This high energy input can be due to feedback inhibition of carbohydrate accumulation on the electron transport chain. An increase in the level of carotenoids as a result of exposure to higher PPFDs or TiO_2 concentrations is a helpful strategy to direct the energy input toward the NPQ. In this way, the photosynthetic apparatus remains adequately protected under conditions of excessively high light energy input.

The rapid light curves illustrate the short-term photosynthetic response to rising light levels. Studying them is a proper way to gain knowledge on overall photosynthetic performance as well as the saturation characteristics of electron transport[49]. In the present study, rapid light curves of both Φ_{PSII} and rETR were assessed. As measuring light intensity increased, Φ_{PSII} decreased whereas rETR increased (Fig. 10). The decline in Φ_{PSII} denotes a limited capacity for photochemical energy usage. In rETR, both the lower increase and the development of a plateau depict the light intensity, where the photosynthetic pathway became limited. Across measurement light levels (100 – 1000 µmol m^{-2} s^{-1} PPFD), leaves cultivated under higher light intensities generally sustained higher Φ_{PSII} and rETR values (Fig. 10). At 75 µmol m^{-2} s^{-1} PPFD during cultivation, TiO_2 nanoparticle spray (100 µmol L^{-1}) tended to sustain higher Φ_{PSII} and rETR values. In accordance, it has been shown that foliar spraying of 100 mg L^{-1} of TiO_2 nanoparticles under low light intensity increased the rate of photosynthesis and yield in cherry tomato plants[30].

In conclusion, radish plants employed two mechanisms under contrasting lighting conditions. In the first mechanism (morphological adaptation), under low light, plants partitioned their biomass toward upper-ground parts which resulted in smaller tubers. Furthermore, plants allocated their biomass toward leaf expansion rather than leaf thickness which was indicated by the high SLA of plants under low light intensity (shade avoidance response). Conversely, plants under high light partitioned most of biomass toward underground parts which resulted in production of bigger tubers. They also produced thicker leaves with limited area to avoid capturing excessive light photons. In the second mechanism (photosynthetic acclimation), plants decreased NPQ and accumulated less carbohydrates under low light condition, while increased NPQ and produced more carbohydrates under high light condition. TiO_2 nanoparticle application mitigate the shade avoidance response under low light intensities, while increased NPQ and reduced electron transport under high light due to higher energy perception (Fig. 12).

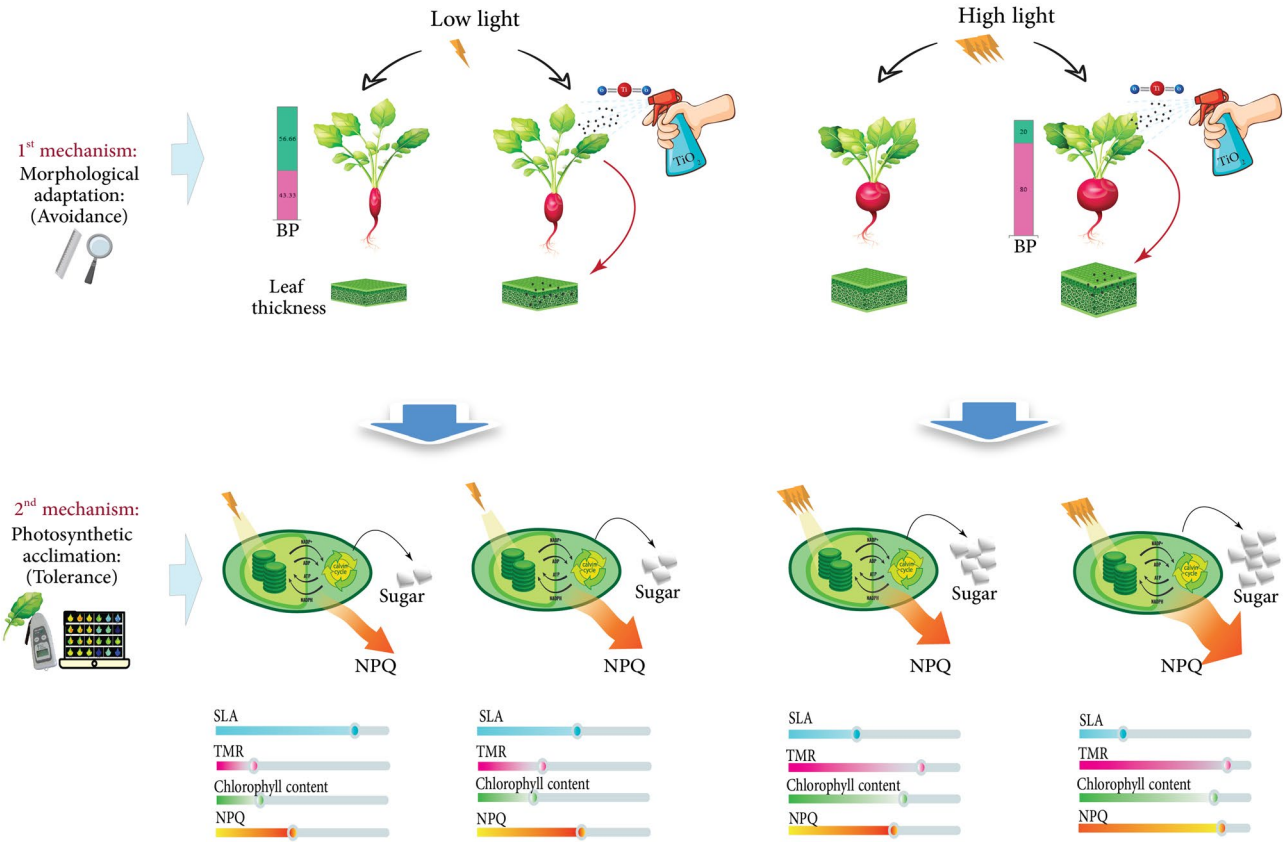

Figure 12. A schematic illustration on the effect of low and high cultivation light intensity and titanium dioxide (TiO_2) nanoparticles application on radish plants. Under low light, plants partitioned less biomass towards the tubers and allocated their biomass toward leaf expansion rather than leaf thickness. Low light-exposed plants decreased NPQ and accumulated less carbohydrates. Conversely, under high light, plants partitioned most of their biomass into the tubers and produced thick leaves with limited area. They increased NPQ and produced more carbohydrates under high light condition. TiO_2 nanoparticle application directed more biomass into the tubers under low light intensities, while increased NPQ under high light condition.

Materials and methods

Plant material and growth conditions. Seeds of radish (*R. raphanistrum*) cv. Cherry Belle were sterilized (3 min) in sodium hypochlorite solution (5%; v/v), and then rinsed (3 min) with distilled water. Seeds were then manually planted in a seedling tray (30 × 18 × 5 cm) filled with a mixture of peat and perlite (1:1, v/v). The sowing depth was kept constant, and seeds were covered with substrate immediately after sowing. At the two-leaf stage, plants were transferred to 2 L pots [diameter (top) × diameter (bottom) × height = 15 × 13 × 15 cm] containing the same mixture. To facilitate drainage, 5 ± 1 g of pebbles (particle size of 16–30 mm) had been earlier placed at the bottom of each pot. Next, 120 pots were equally distributed to four environmentally-controlled growth chambers (l × w × h = 1.5 × 1.0 × 1.3 m) for realizing treatments. A density of 20 plants per m^2 was employed.

Twelve factors (4 light intensities × 3 TiO_2 nanoparticle spray treatments) were applied as a factorial experiment based on a completely randomized design. Each growth chamber included a single light intensity level, which was set at 75, 150, 300 and 600 µmol m^{-2} s^{-1} PPFD for 16 h d^{-1} (06:00–22:00), respectively. In all chambers, light was provided by red (660 nm peak wavelength) and blue (450 nm peak wavelength) LED modules (Parcham Co, Tehran, Iran) with a (red to blue) ratio of 3 to 1. Light intensity was determined by a handy fluorometer (PAR-FluorPen FP 100-MAX, Photon Systems Instruments, Drásov, Czech Republic), while the spectrum was defined by a handy spectrometer (Seconic C7000, Japan).

The remaining environmental variables were identical among the four growth chambers. Day/ night air temperature was set to 26/ 16 °C, and relative air humidity was adjusted to 65–70%. Two ventilation fans (12 V, 0.90A) were installed in each growth chamber to ensure uniform air circulation. Plants were cultivated in a customized liquid culture hydroponic system, by using a modified Hoagland nutrient solution (pH ≈ 5.8; EC ≈ 1.8 dS m^{-1}; detailed composition in Table 2). Growth media moisture was maintained at or near maximum water-holding capacity. To prevent salt accumulation, pots were also irrigated with distilled water twice a week (> 20% drainage).

Plant- and leaf-level measurements were conducted. For leaf-level measurements, sampled leaves had grown under direct light, and were fully-expanded. Replicate leaves were selected from separate plants. To minimize border effects, experimental plants were surrounded by border plants (adjacent to chamber walls) that were not sampled. Samples were collected at the onset of the light period (06:00–07:00 h). Different treatments were always assessed simultaneously. In growth and biomass allocation measurements, the time between sampling and the

Ingredient	Quantity for 1 L of stock solution (g)
Calcium nitrate	97
Potassium nitrate	61
Magnesium sulfate (16% MgO)	25
Mono-potassium phosphate	19
Potassium sulfate	17
Iron EDDHA (6%)	3.723
Mono-ammonium phosphate	1
Borax (11.3% B)	0.383
Zinc sulfate	0.35
Manganese sulfate	0.3
Copper sulfate	0.04
Sodium molybdate (39.6%)	0.024

Table 2. Stock solutions' ingredients employed in the present study. From each stock solution, 10 mL was added to prepare 1 L of nutrient solution.

start of the evaluation did not exceed 15 min. In the remaining evaluations, samples were placed in vials, flash frozen in liquid nitrogen, and transferred to a freezer (− 80 °C) for storage. In all cases, sampling was conducted at the end of the cultivation period, besides the chlorophyll fluorescence evaluation, which was performed 1 d earlier. In all determinations, six replicates were assessed per treatment, besides chlorophyll fluorescence assessments, where nine replicates were evaluated.

Preparation of TiO_2 suspension. The methods used for the synthesis of TiO_2 nanoparticles are Sol–gel route, fame hydrolysis, co-precipitation, impregnation and chemical vapor deposition. Three crystalline phases of titanium dioxide, are anatase (tetragonal), rutile (tetragonal), and brookite (orthorhombic), that brookite has no commercial value[11]. TiO_2 nanoparticles in the anatase form (˃ 99% purity, APS: 10–25 nm, Color: white, Bulk density: 0.24 g/cm^3, True density: 3.9 g/cm^3, PH: 6–6.5) were obtained from a commercial supplier (Iranian Nanomaterial Pioneers Company, Mashhad, Iran). The shape, size and crystal structure of TiO2 nanoparticles were evaluated using SEM, TEM, XRD and FTIR. The Specific surface area (SSA) and pores were analyzed by BET (Brunauer–Emmett–Teller) instrument.

In each light intensity regime, following adaptation (3 d), TiO_2 nanoparticles at different concentrations (0, 50, and 100 µmol L^{-1}) were weekly applied (three times in total) via foliar spray. The suitable concentration range was selected based on both a comprehensive literature survey[20,28,57], and a pre-experiment. Each time before application, the TiO_2 nanoparticles solution was ultrasonically homogenized using a sonicator (UP100H, Hielscher Ultrasonics, Germany)[58–60]. At the time of the first application, plants were still at the two-leaf stage.

Plant growth, morphology, and biomass allocation. The petiole (stalk) length (from the base to the leaf joint), the number of leaves, individual leaf area (one-sided surface area), and plant leaf area were first determined. For leaf area assessment, leaves were scanned (HP Scanjet G4010, Irvine, CA, USA) and then evaluated by using the Digimizer software (version 5.3.5, MedCalc Software, Ostend, Belgium)[21,61].

Following removal of the substrate from the tuber via gentle washing, tuber volume was measured by employing a volume-displacement technique[62,63]. Tubers were suspended in a cylinder filled with water, and tuber volume was then determined by measuring the volume of displaced water.

Leaf and tuber (fresh and dry) masses were also recorded (± 0.01 g; MXX-412; Denver Instruments, Bohemia, NY, USA). For measuring dry weight, samples were placed in a forced-air drying oven for 72 h at 80 °C. By using dry mass, specific leaf area (SLA; leaf area/leaf mass), leaf mass ratio (LMR; leaf mass/plant mass), and tuber mass ratio (TMR; tuber mass/plant mass) were calculated.

Prior to the destructive measurements, plant images were obtained by using a digital camera (Canon EOS M2; Canon Inc., Tokyo, Japan). The plants were manually moved to the image capture station. The imaging station included top and side lighting units (fluorescent tubes; Pars Shahab Lamp Co., Tehran, Iran). The camera-to-plant distance was maintained constant. One image (RGB) was obtained per plant.

Leaf chlorophyll and carotenoid content. Samples (0.1 g) were homogenized with the addition of 10 mL of 100% acetone. The extract was then centrifuged (14,000 g for 15 min), and the supernatant was collected. Since chlorophyll is light sensitive, the extraction took place in a dark room[58,59]. The obtained extract was subjected to reading on a spectrophotometer (Optizen pop, Mecasys Co. Ltd. Daejeon, Korea). Total chlorophyll and carotenoid contents were calculated according to Lichtenthaler and Wellburn[64].

Leaf total soluble carbohydrates content. Colorimetric quantification of leaf total soluble carbohydrates (i.e., reducing and non-reducing sugars) content was performed[65]. Shortly before analysis (< 30 min), the anthrone reagent was prepared under darkness by dissolving 0.1 g of anthrone (0.2%) in 100 mL of concentrated sulfuric acid (98%). Sample (0.1 g) and anthrone reagent (1 mL) were loaded in tubes, which were placed in

Category	Abbreviation	Definition	Equation
Basic parameters	F_0	Minimum fluorescence, when all PSII reaction centers are open (O-step of OJIP transient)	$F_{50\mu s}$
	F_J	Fluorescence intensity at the J-step (2 ms) of OJIP	F_{2ms}
	F_I	Fluorescence intensity at the I-step (30 ms) of OJIP	F_{30ms}
Fluorescence parameters	F_m	Maximum fluorescence, when all PSII reaction centers are closed (P-step of OJIP transient)	$F_{1s} = F_p$
	F_v	Variable fluorescence of the dark-adapted sample	$F_m - F_0$
	V_J	Relative variable fluorescence at time 2 ms (J-step) after start of actinic light pulse	$(F_J - F_0)/(F_m - F_0)$
	V_I	Relative variable fluorescence at time 30 ms (I-step) after start of actinic light pulse	$(F_{30ms} - F_0)/(F_m - F_0)$
	F_v/F_m	Maximal quantum yield of PSII photochemistry	$1 - (F_0/F_m) = (F_m - F_0)/F_m = \varphi_{P0} = TR_0/ABS$
Quantum yields and efficiencies/probabilities	φ_{E0}	The quantum yield of electron transport	$[1 - (F_0/F_m)](1 - V_J) = ET_0/ABS$
	φ_{D0}	Quantum yield of energy dissipation	F_0/F_m
	φ_{PAV}	Average (from time 0 to t_{FM}) quantum yield for primary photochemistry	$\varphi_{P0}(1 - V_J) = \varphi_{P0}(S_M/t_{FM})$
Specific energy fluxes (per Q_A reducing PSII reaction center)	ABS/RC	The specific energy fluxes per reaction center for energy absorption	$M_0(1/V_J)(1/\varphi_{P0})$
	TR_0/RC	Trapped energy flux (leading to Q_A reduction) per reaction center	$M_0(1/V_J)$
	ET_0/RC	Electron transport flux (further than Q_A^-) per reaction center	$M_0(1/V_J)(1 - V_J)$
	DI_0/RC	Dissipated energy flux	$(ABS/RC) - (TR_0/RC)$
Performance indices (products of terms expressing partial potentials at steps of energy bifurcations)	PI_{ABS}	Performance index for the photochemical activity	$[(\gamma RC/1 - \gamma RC)(\varphi_{P0}/1 - \varphi_{P0})(\psi_{E0}/1 - \psi_{E0})]$
	NPQ	Non-photochemical quenching	$(F_m/F_m') - 1$
Rapid light curve as a function of PPFD	Φ_{PSII}	Effective quantum yield of PSII	$\Delta F/F_m' = (F_m' - F)/F_m'$
	rETR	Relative electron transport rate	$\Phi_{PSII} \times PPFD \times 0.5 \times 0.84$

Table 3. Abbreviations, definitions and formulas of the chlorophyll fluorescence parameters assessed in the current study.

a water bath (90 °C for 15 min), cooled (0 °C for 5 min), and vortexed (1 min). Before reading, a heating step (20 min) to room temperature (25 °C) was performed. The absorbance was measured at 620 nm with a spectrophotometer (Optizen pop, Mecasys Co. Ltd. Daejeon, Korea). A standard curve based on a series of known glucose concentrations was prepared.

Maximum quantum yield of photosystem II (PSII). As a sensitive indicator of photosynthetic performance, dark-adapted values of the maximum quantum yield of PSII (F_v/F_m; equation and explanation in Table 3) were non-invasively recorded in leaves of each treatment[22,37,63]. Measurements were performed by using a portable imaging fluorometer (Handy FluorCam FC 1000-H, Photon Systems Instruments, Drásov, Czech Republic). Before taking measurements, samples were dark-adapted (≥ 20 min). Then, F_v/F_m was evaluated by a custom-made protocol[21,23], where leaves were exposed to short flashes followed by long saturated light pulses (3900 µmol m^{-2} s^{-1} PPFD) to cause a reduction in the primary quinone acceptor of PSII.

Polyphasic chlorophyll fluorescence transient (O–J–I–P) evaluation. A polyphasic chlorophyll fluorescence induction curve (O–J–I–P-transient) was obtained in the attached leaves of each treatment. By employing this test, the shape changes of the O–J–I–P transient are quantitatively translated to a set of parameters (see Table 3), which relate to the in vivo adaptive behavior of the photosynthetic apparatus (especially PSII) to the growth environment[25,26]. Measurements were conducted by using a PAR- FluorPen FP 100-MAX (Photon Systems Instruments, Drásov, Czech Republic) following dark adaptation (≥ 20 min). The employed light intensity (3900 µmol m^{-2} s^{-1} PPFD) was sufficient to generate maximal fluorescence in all treatments.

Following dark adaptation, leaves exhibit a polyphasic chlorophyll fluorescence rise during the first second of illumination. The fluorescence transient, plotted on a logarithmic time scale, typically includes the following phases: O to J, J to I, and I to P. F_0 was measured at 50 µs, fluorescence intensity at J-step was assessed at 2 ms, and fluorescence intensity at I-step was evaluated at 30 ms[39,66].

Non-photochemical quenching. Another set of dark-adapted attached leaves were used to determine non-photochemical quenching (NPQ; equation and description in Table 3) by using a PAR-FluorPen FP 100-MAX (Photon Systems Instruments, Drásov, Czech Republic). Calculations were performed by using the FluorPen software (v. 7; Photon Systems Instruments, Drásov, Czech Republic).

Rapid light curve of effective quantum yield of PSII and electron transport rate. The rapid light curve of effective quantum yield of PSII (Φ_{PSII}; equation and description in Table 3) was determined with a handy fluorometer (PAR-FluorPen FP 100-MAX, Photon Systems Instruments, Drásov, Czech Republic). The dark-adapted leaves were exposed to a gradual increase of actinic blue light illumination in six steps (0, 100, 200, 300, 500 and 1000 µmol m^{-2} s^{-1} PPFD). Each illumination step was separated by 10 s intervals. Illuminating the saturating flash required 0.8 s. Data were analyzed by using the FluorPen software (v. 7; Photon Systems Instruments, Drásov, Czech Republic). Relative electron transport rate (rETR; equation and description in Table 3) was also calculated[54].

Statistical analysis. Data were subjected to analysis of variance using SAS software (v. 9.4, SAS Institute Inc., Cary, NC, USA). Data were firstly tested for normality (Shapiro–Wilk test) and homogeneity of variances (Levene's test). A split-plot design was employed, with cultivation light intensity (75, 150, 300 and 600 µmol m^{-2} s^{-1} PPFD) as the main factor, and TiO_2 nanoparticles concentration (0, 50, and 100 µmol L^{-1}) as the split factor. Treatment effects were tested at a 5% probability level and mean separation was carried out using the least significant differences based on Duncan's multiple range test ($P \leq 0.05$).

Data availability

The main data are contained within the article. Data are available upon request from the corresponding author.

Received: 13 July 2022; Accepted: 28 March 2023
Published online: 11 April 2023

References

1. Meyfroidt, P. Trade-offs between environment and livelihoods: Bridging the global land use and food security discussions. *Glob. Food Sec.* **16**, 9–16 (2018).
2. Simkin, A. J., López-Calcagno, P. E. & Raines, C. A. Feeding the world: Improving photosynthetic efficiency for sustainable crop production. *J. Exp. Bot.* **70**, 1119–1140 (2019).
3. Godfray, H. C. J. *et al.* Food security: The challenge of feeding 9 billion people. *Science* **327**, 812–818 (2010).
4. Xie, H., Huang, Y., Chen, Q., Zhang, Y. & Wu, Q. Prospects for agricultural sustainable intensification: A review of research. *Land* **8**, 157 (2019).
5. Paschalidis, K. *et al.* Pilot cultivation of the vulnerable cretan endemic verbascum arcturus l. (scrophulariaceae): Effect of fertilization on growth and quality features. *Sustain.* **13**, 14030 (2021).
6. Moosavi-Nezhad, M., Salehi, R., Aliniaeifard, S., Winans, K. S. & Nabavi-Pelesaraei, A. An analysis of energy use and economic and environmental impacts in conventional tunnel and LED-equipped vertical systems in healing and acclimatization of grafted watermelon seedlings. *J. Clean. Prod.* **361**, 132069 (2022).
7. Sarkar, S. *et al.* Management of crop residues for improving input use efficiency and agricultural sustainability. *Sustain.* **12**, 1–24 (2020).
8. Shang, Y. *et al.* Applications of nanotechnology in plant growth and crop protection: A review. *Molecules* **24**, 2558 (2019).
9. Shi, H., Magaye, R., Castranova, V. & Zhao, J. Titanium dioxide nanoparticles: A review of current toxicological data. *Part. Fibre Toxicol.* **10**, 1–33 (2013).
10. Irshad, M. A. *et al.* Synthesis, characterization and advanced sustainable applications of titanium dioxide nanoparticles: A review. *Ecotoxicol. Environ. Saf.* **212**, 111978 (2021).
11. Waghmode, M. S., Gunjal, A. B., Mulla, J. A., Patil, N. N. & Nawani, N. N. Studies on the titanium dioxide nanoparticles: Biosynthesis, applications and remediation. *SN Appl. Sci.* **1**, 310 (2019).
12. Fanourakis, D. *et al.* Stomatal anatomy and closing ability is affected by supplementary light intensity in rose (Rosa hybrida L.). *Hortic. Sci.* **46**, 81–89 (2019).
13. Sørensen, H. K. *et al.* Using artificial lighting based on electricity price without a negative impact on growth, visual quality or stomatal closing response in Passiflora. *Sci. Hortic.* **267**, 109354 (2020).
14. Moradi, S. *et al.* Blue light improves photosynthetic performance and biomass partitioning toward harvestable organs in saffron (Crocus sativus L.). *Cells* **10**, 1994 (2021).
15. Ashrostaghi, T. *et al.* Light intensity: The role player in cucumber response to cold stress. *Agronomy* **12**, 201 (2022).
16. Esmaeili, S. *et al.* Elevated light intensity compensates for nitrogen deficiency during chrysanthemum growth by improving water and nitrogen use efficiency. *Sci. Rep.* **12**, 10002 (2022).
17. Ghorbanzadeh, P. *et al.* Dependency of growth, water use efficiency, chlorophyll fluorescence, and stomatal characteristics of lettuce plants to light intensity. *J. Plant Growth Regul.* **40**, 2191–2207 (2021).
18. Collado, C. E. & Hernández, R. Effects of light intensity, spectral composition, and paclobutrazol on the morphology, physiology, and growth of petunia, geranium, pansy, and dianthus ornamental transplants. *J. Plant Growth Regul.* 1–18 (2022).
19. Gómez, C. *et al.* Controlled environment food production for urban agriculture. *HortScience* **54**, 1448–1458 (2019).
20. Choi, H. G. *et al.* Effects of foliar fertilization containing titanium dioxide on growth, yield and quality of strawberries during cultivation. *Hortic. Environ. Biotechnol.* **56**, 575–581 (2015).
21. Moosavi-Nezhad, M. *et al.* Blue light improves photosynthetic performance during healing and acclimatization of grafted watermelon seedlings. *Int. J. Mol. Sci.* **22**, 8043 (2021).
22. Yang, L. *et al.* Contrary to red, blue monochromatic light improves the bioactive compound content in broccoli sprouts. *Agronomy* **11**, 2139 (2021).
23. Seifikalhor, M. *et al.* The regulatory role of γ-aminobutyric acid in chickpea plants depends on drought tolerance and water scarcity level. *Sci. Rep.* **12**, 7034 (2022).
24. Moosavi-Nezhad, M., Alibeigi, B., Estaji, A., Gruda, N. S. & Aliniaeifard, S. Growth, biomass partitioning, and photosynthetic performance of chrysanthemum cuttings in response to different light spectra. *Plants* **11**, 3337 (2022).
25. Kalaji, H. M. *et al.* Frequently asked questions about chlorophyll fluorescence, the sequel. *Photosynth. Res.* **132**, 13–66 (2017).
26. Seif, M. *et al.* Monochromatic red light during plant growth decreases the size and improves the functionality of stomata in chrysanthemum. *Funct. Plant Biol.* https://doi.org/10.1071/FP20280 (2021).
27. Moradi, S. *et al.* Monochromatic blue light enhances crocin and picrocrocin content by upregulating the expression of underlying biosynthetic pathway genes in saffron (Crocus sativus L.). *Front. Hortic.* **1**, (2022).
28. Chahardoli, A., Sharifan, H., Karimi, N. & Kakavand, S. N. Uptake, translocation, phytotoxicity, and hormetic effects of titanium dioxide nanoparticles (TiO_2NPs) in Nigella arvensis L. *Sci. Total Environ.* **806**, 151222 (2022).

29. Hussain, S. *et al.* Changes in morphology, chlorophyll fluorescence performance and Rubisco activity of soybean in response to foliar application of ionic titanium under normal light and shade environment. *Sci. Total Environ.* **658**, 626–637 (2019).
30. Choi, H. G. Effect of TiO_2 nanoparticles on the yield and photophysiological responses of cherry tomatoes during the rainy season. *Horticulturae* **7**, 563 (2021).
31. Lastochkina, O. *et al.* Novel approaches for sustainable horticultural crop production: Advances and prospects. *Horticulturae* **8**, 910 (2022).
32. Zhao, X. *et al.* Exploring engineering reduced graphene oxide-titanium dioxide (RGO-TiO2) nanoparticles treatment to effectively enhance lutein biosynthesis with Chlorella sorokiniana F31 under different light intensity. *Bioresour. Technol.* **348**, 126816 (2022).
33. Levine, L. H. *et al.* Quality characteristics of the radish grown under reduced atmospheric pressure. *Adv. Sp. Res.* **41**, 754–762 (2008).
34. Viana, M. M., Soares, V. F. & Mohallem, N. D. S. Synthesis and characterization of TiO_2 nanoparticles. *Ceram. Int.* **36**, 2047–2053 (2010).
35. Raliya, R., Nair, R., Chavalmane, S., Wang, W.-N. & Biswas, P. Mechanistic evaluation of translocation and physiological impact of titanium dioxide and zinc oxide nanoparticles on the tomato (Solanum lycopersicum L.) plant. *Metallomics* **7**, 1584–1594 (2015).
36. Zou, J. *et al.* Lettuce growth, morphology and critical leaf trait responses to far-red light during cultivation are low fluence and obey the reciprocity law. *Sci. Hortic.* **289**, 104555 (2021).
37. Chen, Y. *et al.* Low UVA intensity during cultivation improves the lettuce shelf-life, an effect that is not sustained at higher intensity. *Postharvest Biol. Technol.* **172**, 111376 (2021).
38. Lichtenthaler, H. K., Ač, A., Marek, M. V., Kalina, J. & Urban, O. Differences in pigment composition, photosynthetic rates and chlorophyll fluorescence images of sun and shade leaves of four tree species. *Plant Physiol. Biochem.* **45**, 577–588 (2007).
39. Baker, N. R. Chlorophyll fluorescence: A probe of photosynthesis in vivo. *Annu. Rev. Plant Biol.* **59**, 89–113 (2008).
40. Maxwell, K. & Johnson, G. N. Chlorophyll fluorescence—a practical guide. *J. Exp. Bot.* **51**, 659–668 (2000).
41. Esmaili, M. *et al.* Assessment of adaptive neuro-fuzzy inference system (ANFIS) to predict production and water productivity of lettuce in response to different light intensities and CO_2 concentrations. *Agric. Water Manag.* **258**, 107201 (2021).
42. Hosseinzadeh, M., Aliniaeifard, S., Shomali, A. & Didaran, F. Interaction of light intensity and CO_2 concentration alters biomass partitioning in chrysanthemum. *J. Hortic. Res.* **29**, 45–56 (2021).
43. Esmaili, M. *et al.* CO_2 enrichment and increasing light intensity till a threshold level, enhance growth and water use efficiency of lettuce plants in controlled environment. *Not. Bot. Horti Agrobot. Cluj-Napoca* **48**, 2244–2262 (2020).
44. Hazrati, S., Tahmasebi-Sarvestani, Z., Modarres-Sanavy, S. A. M., Mokhtassi-Bidgoli, A. & Nicola, S. Effects of water stress and light intensity on chlorophyll fluorescence parameters and pigments of Aloe vera L. *Plant Physiol. Biochem.* **106**, 141–148 (2016).
45. Kalaji, H. M. *et al.* Chlorophyll a fluorescence as a tool to monitor physiological status of plants under abiotic stress conditions. *Acta Physiol. Plant.* **38**, 102 (2016).
46. Oukarroum, A., Madidi, S. E., Schansker, G. & Strasser, R. J. Probing the responses of barley cultivars (Hordeum vulgare L.) by chlorophyll a fluorescence OLKJIP under drought stress and re-watering. *Environ. Exp. Bot.* **60**, 438–446 (2007).
47. Martins, J. P. R., Schimildt, E. R., Alexandre, R. S., Falqueto, A. R. & Otoni, W. C. Chlorophyll a fluorescence and growth of Neoregelia concentrica (Bromeliaceae) during acclimatization in response to light levels. *Vitr. Cell. Dev. Biol. - Plant* **51**, 471–481 (2015).
48. Rapacz, M., Sasal, M., Kalaji, H. M. & Kościelniak, J. Is the OJIP test a reliable indicator of winter hardiness and freezing tolerance of common wheat and triticale under variable winter environments?. *PLoS ONE* **10**, e0134820 (2015).
49. Shabbir, A. *et al.* Efficacy of TiO2 nanoparticles in enhancing the photosynthesis, essential oil and khusimol biosynthesis in Vetiveria zizanioides L. *Nash. Photosynthetica* **57**, 599–606 (2019).
50. Gao, F. *et al.* Mechanism of nano-anatase TiO 2 on promoting photosynthetic carbon reaction of spinach: Inducing complex of rubisco-rubisco activase. *Biol. Trace Elem. Res.* **111**, 239–253 (2006).
51. Azmat, R., Altaf, I. & Moin, S. The reflection of the photocatalytic properties of TiO 2 nanoparticles on photosynthetic activity of Spinacia oleracea plants. *Pak. J. Bot* **52**, 1229–1234 (2020).
52. Fu, W., Li, P. & Wu, Y. Effects of different light intensities on chlorophyll fluorescence characteristics and yield in lettuce. *Sci. Hortic. (Amsterdam)* **135**, 45–51 (2012).
53. Pinnola, A. *et al.* Zeaxanthin binds to light-harvesting complex stress-related protein to enhance nonphotochemical quenching in Physcomitrella patens. *Plant Cell* **25**, 3519–3534 (2013).
54. Ralph, P. J. & Gademann, R. Rapid light curves: A powerful tool to assess photosynthetic activity. *Aquat. Bot.* **82**, 222–237 (2005).
55. Jahns, P. & Holzwarth, A. R. The role of the xanthophyll cycle and of lutein in photoprotection of photosystem II. *Biochim. Biophys. Acta - Bioenerg.* **1817**, 182–193 (2012).
56. Lacour, T., Babin, M. & Lavaud, J. Diversity in Xanthophyll Cycle Pigments Content and Related Nonphotochemical Quenching (NPQ) Among Microalgae: Implications for Growth Strategy and Ecology. *J. Phycol.* **56**, 245–263 (2020).
57. Lian, J. *et al.* Foliar spray of TiO_2 nanoparticles prevails over root application in reducing Cd accumulation and mitigating Cd-induced phytotoxicity in maize (Zea mays L.). *Chemosphere* **239**, 124794 (2020).
58. Ahmadi-Majd, M., Mousavi-Fard, S., Rezaei Nejad, A. & Fanourakis, D. Carbon nanotubes in the holding solution stimulate flower opening and prolong vase life in carnation. *Chem. Biol. Technol. Agric.* **9**, 15 (2022).
59. Ahmadi-Majd, M., Rezaei Nejad, A., Mousavi-Fard, S. & Fanourakis, D. Postharvest application of single, multi-walled carbon nanotubes and nanographene oxide improves rose keeping quality. *J. Hortic. Sci. Biotechnol.* **97**, 346–360 (2022).
60. Vatankhah, A., Reezi, S., Izadi, Z., Ghasemi-Varnamkhasti, M. & Motamedi, A. Development of an ultrasensitive electrochemical biosensor for detection of Agrobacterium tumefaciens in Rosa hybrida L. *Measurement* **187**, 110320 (2022).
61. Yousefzadeh, K. *et al.* Joint effects of developmental stage and water deficit on essential oil traits (content, yield, composition) and related gene expression: A case study in two thymus species. *Agronomy* **12**, 1008 (2022).
62. Javadi Asayesh, E. *et al.* Supplementary light with increased blue fraction accelerates emergence and improves development of the inflorescence in aechmea, guzmania and vriesea. *Horticulturae* **7**, 485 (2021).
63. Estaji, A., Kalaji, H. M., Karimi, H. R., Roosta, H. R. & Moosavi-Nezhad, S. M. How glycine betaine induces tolerance of cucumber plants to salinity stress?. *Photosynthetica* **57**, 753–761 (2019).
64. Lichtenthaler, H. K. & Wellburn, A. R. Determinations of total carotenoids and chlorophylls a and b of leaf extracts in different solvents. *Biochem. Soc. Trans.* **11**, 591–592 (1983).
65. Yemm, E. W. & Willis, A. J. The estimation of carbohydrates in plant extracts by anthrone. *Biochem. J.* **57**, 508–514 (1954).
66. Zushi, K., Kajiwara, S. & Matsuzoe, N. Chlorophyll a fluorescence OJIP transient as a tool to characterize and evaluate response to heat and chilling stress in tomato leaf and fruit. *Sci. Hortic.* **148**, 39–46 (2012).

Acknowledgements

The authors gratefully acknowledge the laboratory staff for their contributions, continued diligence, and dedication to their craft.

Author contributions

Conceptualization, A.V., M.M-N, S.Al., and D.F.; data curation, A.V., S.Ab., M.M-N., and S.R.; formal analysis, A. V., M.M-N.; investigation, A. V., S.Ab., Z.M., M.M-N.; project administration, S.Al.; supervision, S.Al., S.R. and D.F.; funding, A. V, S. Al., and S.R.; visualization, M.M-N; writing—original draft, D.F.; writing—review and editing, S.Al., M.M-N., G.T., and D.F. All authors have read and agreed to the published version of the manuscript.

Funding

This research was financed by a research grant from the Ministry of Science, Research and Technology of Iran as a post-doctoral project to Akram Vatankhah (No: 5547981).

Competing interests

The authors declare no competing interests.

Additional information

Correspondence and requests for materials should be addressed to S.A.

Reprints and permissions information is available at www.nature.com/reprints.

Publisher's note Springer Nature remains neutral with regard to jurisdictional claims in published maps and institutional affiliations.